FIBER REINFORCED SOY-BASED POLYURETHANE SPRAY FOAM INSULATION. PART 2: THERMAL AND MECHANICAL PROPERTIES

Ruijun Gu, Mustafa Khazabi, and Mohini Sain *

Bio-based polyurethane (PU) spray foam insulation was prepared with soy polyol. The effects of adding wood fiber and water on the thermal and mechanical properties of the insulations were studied. The decomposition temperature (*Td*) of the foams increased with fiber reinforcement due to a higher degree of crosslinking. Alternatively, different fiber length contributed to different crosslinking. In addition, the neat foams, which didn't contain wood fibers, had exceptional thermal stability with the increase of the amount of H_2O by forming more stable polyurea adducts. In addition, PU spray foam blown with a larger content of H_2O had higher compressive strength by forming a stiffer phase. Still, PU spray foam reinforced with fiber also had superior compressive strength due to the fiber framing into the foam struts. The effect of the fiber length on the compressive strength was evaluated. The degree of complex networks was influenced by the fiber length. However, the tensile strength was weakened with the addition of wood fiber.

Keywords: Biofoam, Insulation; Polyurethane; Spray foam; Soybean oil; Wood fiber

Contact information: Faculty of Forestry, University of Toronto, Toronto, ON, M5S 3B3 CANADA
**Corresponding author email: m.sain@utoronto.ca*

INTRODUCTION

Bio-based foams reduce risk from unpredictable and increasable prices of fossil fuel; such materials have moved into the mainstream for the construction building industry (Pollack 2004). Sprayed PU foam is mostly used in construction (Bomberg and Kumaran 1999) due to its effective energy saving (Moore and Ference 1998) and improved sound abatement (Falke et al. 2001). New sustainable bio-based PU spray foams are made from renewable bio-sources (Meyer 2011), thus consuming less energy and reducing carbon footprints. Soy-based PU spray foam is being driven by large soybean output in North America (USDA 2011). Meanwhile, the agricultural industry will thrive by the growing demand for soy. Furthermore, soy-based foam could achieve higher thermal and dimensional stability than petroleum-based foams due to containing triglyceride structures (Javni et al. 2004).

Though PU foams based on vegetable oils have been reported (Banik and Sain 2008; Petrović 2008), there are no records of PU spray foams, especially for PU spray foams reinforced with wood fiber. Due to wood fiber being rich in –OH groups for potential reaction to –NCO groups of isocyanates, it would be interesting to study the thermal and mechanical properties of PU spray foam in the presence of wood fiber, in addition to the cell morphologies considered in Part 1 (Khazabi et al. 2011).

EXPERIMENTAL

Materials and Methods

Soy-based Polyol (Soyol)

Soyol was prepared from soybean oil by adding hydroxyls at the unsaturated sites of its abundant triglycerides structures. Low odor Soyol® 2102 was donated by Urethane Soy Systems (Volga, South Dakota, USA). It is the 5th generation of polyol made using soybean oil. Its bio-renewable content is as high as 98%, as reported by ASTM D 6866. Its hydroxyl number was 63 mg KOH/g according to ASTM D4274-99 with the viscosity of 2181 cps at 25ºC. Its moisture is less than 0.01% according to the data by the supplier.

Isocyanate

Polymeric diphenylmethane-diisocyanate (PMDI) having 31.5% NCO content was donated by Huntsman and used to produce sprayed foams. Its functionality was 2.7, as provided by the supplier.

Wood pulp fiber

Steam explosion pulp of trembling aspen (high energy, 8 bar pressure) was received from Forintek Canada Corp (Point-Claire, Quebec, Canada). This air-dried industrial aspen Chemical Thermal Mechanical Pulp (CTMP) was cut and screened into 20-35, 35-70, 70-100, 100-140, 140-200, and 200-325 mesh sizes, respectively. Six select fibers were introduced into PU spray foams as natural filler. This unbleached CTMP fiber imparts a dark-brown color to the PU biofoam.

Catalysts

Diamine was used as a foaming catalyst, which was received from Sigma Chemical Company. Tertiary amine, donated by Air Products and Chemicals, Inc. (Allentown, Pennsylvania, USA), was used as a gelling catalyst.

Surfactant

Polysiloxane family based surfactant was used to achieve superior cell structures; samples were donated by Air Products and Chemicals, Inc.

Blowing agent

Distilled water was used as a blowing agent to generate foams; this was prepared in our lab.

Foam Preparation and Evaluation

PU spray foams were prepared by a free-rise method according to the formulations listed in Table 1. The amount of pulp fiber used was in terms of 100 parts of soyol. The soyol was manually mixed with the additives (catalysts, surfactant and H_2O) at ambient temperature for 5 minutes, and then PMDI was added and mixed for another 20 seconds. Afterwards, the resultant mixture was quickly transferred into a mold for foaming to get neat PU spray foams. For the PU spray foams in presence of wood fiber, wood fiber was pre-mixed with soyol for 20 minutes to soak completely. The processes of the addition of the additives and foaming were same to neat foams. Finally, all the PU spray foams were kept at the room temperature overnight to be well post-cured.

According to our observation, wood fiber can delay the urethane reaction in particular for CTMP fiber from their longer foaming time.

Table 1. Formulations for PU Spray Foam Insulation

Materials		Parts by weight, php	
		Neat PU spray foam	PU-Fiber spray foam
Soyol	Soyol® 2102	100	100
Catalyst	Diamine	1.33	1.33
	Tertiary amine	2.0	2.0
Surfactant	Polysiloxane	0.67	0.67
Blowing agent	H_2O	4.7; 5.3; 6.7; 8.0	6.7
PMDI	NCO index	120	120
Wood fiber	35-70 mesh	---	10; 20†; 30; 40; 50; 60

† Six select fibers were formulated

Fiber Quality Analysis (FQA)

The length of the original fiber was measured by OpTest Fiber Quality Analyzer (OpTest equipment Inc., Hawkesburg, Canada) according to TAPPI T271. 5000 fibers were evaluated to compute an arithmetic mean fiber length. Each sample was tested twice.

Scanning Electron Microscope (SEM) Investigation

Sample stub with thin foam slab was surface metalized by a sputter-coating (BOT 341F) with evaporated gold (in 4nm thickness), and then was carried out by SEM (Hitachi S-2500, Hitachi High Technologies Inc., Tokyo, Japan) at an acceleration voltage of 15kV.

Mechanical Properties

Preparation of ASTM specimens

All the foams were conditioned at 23^{o}C and 45% relative humidity, and then the foam slabs were extracted from a sawing machine and polished with a sanding machine. The length, width and thickness were measured after polishing. The thickness is along the foam rise direction.

Mechanical tests

At least 6 type C specimens (5cm×5cm×3cm) were used for the tensile strength test using a Zwick universal testing machine (Zwick/Z100, Zwick GmbH & Co. KG, Germany) according to ASTM D1623-09 under 23^{o}C and 45% relative humidity (Fig. 1). The rate of crosshead movement was 1.3mm/min.

More than 15 specimens (5cm×5cm×3cm) were tested for compressive strength using an Instron universal testing machine (Model 3367, Instron) according to ASTM D1621-04a under 23°C and 45% relative humidity. The rate of crosshead movement was 2.5mm/min, and the value at 10% deformation was recorded as compressive strength.

Fig. 1. Tensile test of PU spray foams

Thermal Analysis

Thermal analyses for PU spray foams were performed with a thermogravimetric analyzer (TGA Q500) of TA Instruments. Runs of TGA were conducted in the ramp mode from room temperature to 700°C under air condition at 60mL/min flow rate. The heating rate was 10°C/min. Sample weights of TGA were approximately 5 mg in its original state.

Runs of DSC were performed in the temperature range of -60 to 200°C under nitrogen protection at 50mL/min flow rate. The heating rate was 10°C/min in the ramp mode. Samples weights of DSC were approximately 6 mg after fractured in liquid nitrogen.

RESULTS AND DISCUSSION

It has been reported that natural fiber can affect the mechanical properties of PU microfoams (Silva et al. 2010). Although PU spray foam is definitely different from PU microfoams due to its quick expansion and fast dry-time, the influences of wood fiber were expected to impact sprayed foam quality. The average length of 6 classified fibers is shown in Fig. 2. The 6 select fibers had same width due to cutting the same original fiber source. Obviously, fibers in high mesh categories had short length, which were more like particles rather than fibers. Thermal and mechanical properties were investigated after the select fibers were introduced into sprayed PU foam, respectively.

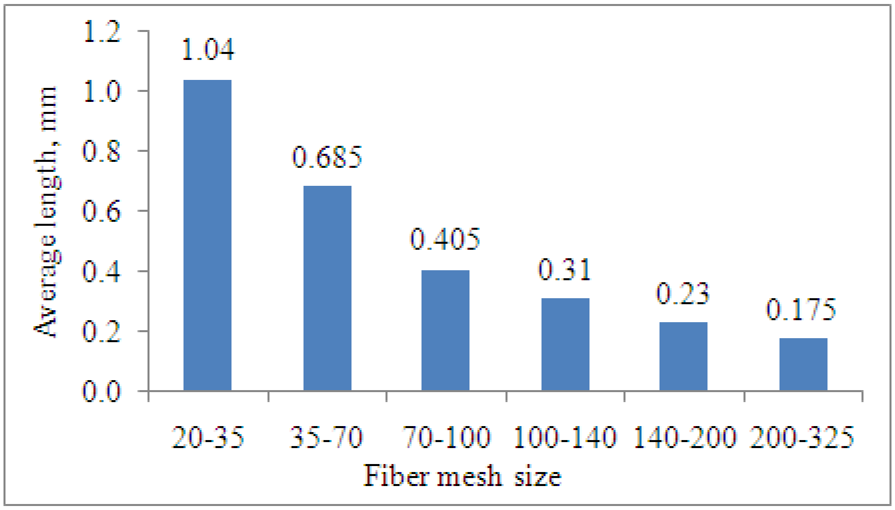

Fig. 2. Average fiber length of select fibers

Thermal Properties of PU Spray Foams

DSC analyses of foam samples were performed to evaluate the effects of wood fiber and blowing agent on foaming. The typical DSC curve of PU spray foam with fiber introduced, which combined the DSC behaviors of pure fiber and neat spray foam, is shown in Fig. 3. Both beta and glass transition temperatures observed from DSC analyses are reported in Fig. 4. Though the DSC trace showed a decreased beta transition with the increase of H_2O or wood fiber (Fig. 4a and b), the identifications were absolutely different. The increase of the amount of H_2O can generate more stiff urea adducts during the reaction of –NCO groups. Rigid urea structures had difficult movement of molecules, exhibiting high T_g temperature as shown in Fig. 4a'. The T_g increased linearly with the amount of H_2O.

In general, the –OH groups of wood fiber would react with –NCO groups of PMDI. The beta transition of PU spray foam in the presence of fiber decreased due to the reaction, leading to conformational changes in the side groups of the matrix backbone (Fig. 4b). This reaction led to additional barriers to free segmental motions. In our study, the T_g shifted to a high temperature from 57ºC up to 85ºC, with additional reaction of wood fiber with –NCO (Fig. 4b'). Similar to the function of H_2O, the increase of T_g was also in linear proportion with the amount of fiber.

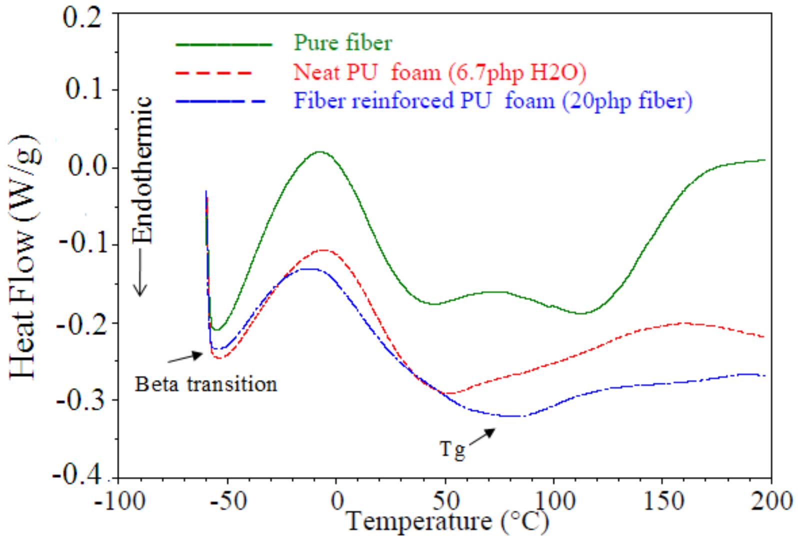

Fig. 3. Typical DSC curves of PU spray foams

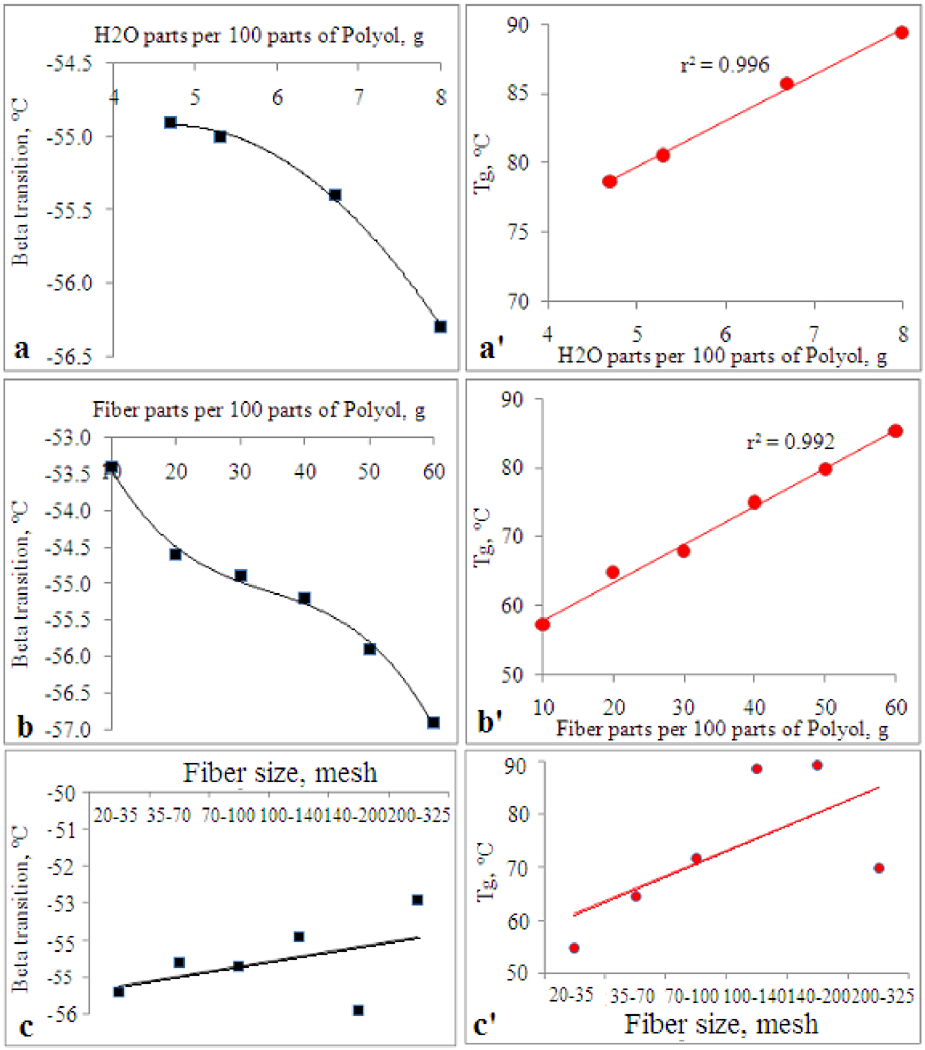

Fig. 4. Effect of the H_2O and fiber on DSC behaviors of PU spray foams

Unlike the functions of H_2O and fiber amount, the fiber size had different behavior on beta transition. Shorter fibers probably formed shorter side groups rather than long molecular chains. It is known that the beta transition is related to the molecules of polyol chains and side chain backbones. It was reasonable to demonstrate high beta transition with the decrease of fiber size due to the formation of shorter side chains. This estimation was verified by the experimental result as shown in Fig. 4c. Though shorter fibers might generate shorter side groups amidst the foam matrix, shorter fiber containing more fiber ends can produce more bonds at these ends (Hsueh 1989). More chemical formations between the fibers and –NCO groups caused high limitation of segmental rotation exhibiting higher T_g, as shown in Fig. 4c'.

Effect of H_2O on cell thermal properties

Although this spray-on material had a skin, the quality of the skin was not controllable. As well, we studied the thermal properties of the foam core. The cell structure had an important effect on foam thermal behavior. TGA analyses of foam samples have been carried out to justify the effect of H_2O concentration as shown in Fig. 5. The thermal degradation temperatures observed from TGA curve are reported in Table 2.

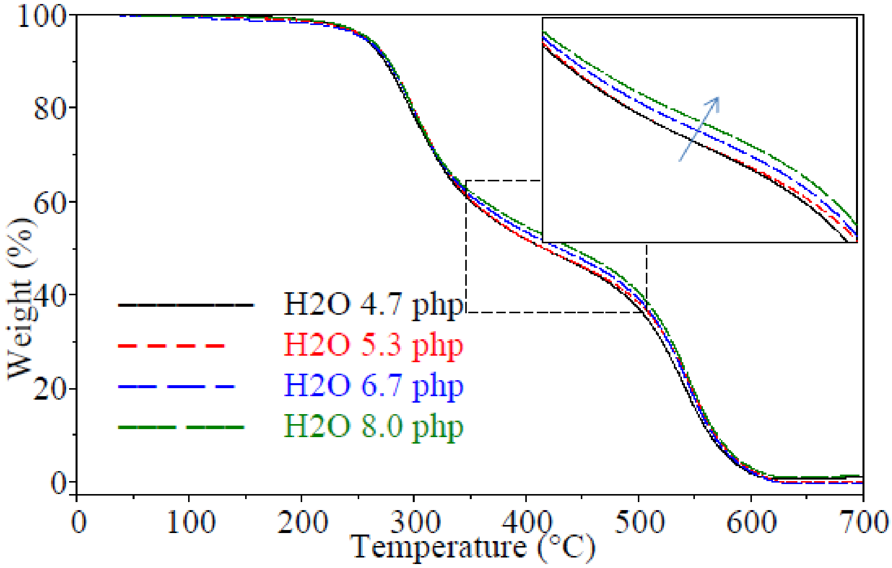

Fig. 5. Effect of H_2O on thermal behavior of PU spray foams

The decomposition temperature (T_d) was correlated with increasing H_2O. Urea formation was a dominant factor in the H_2O-blown PU foam, especially during initial stages of foam rise (Li et al. 2006; Grünbauer et al. 1992). This finding was supported by the data in Table 2. A typical decomposition curve of PU foam with two distinct steps is shown in Fig. 5. Urethane formations were broken down at lower temperature (first stage) with the evolution of isocyanate and alcohol, leading to collapse of the cellular structure (Saber et al. 2010). Polyurea and polybiuret linkages were cleaved at high temperature (second stage) by forming complex degraded products in general. The T_d at 5% weight loss (T_{d5}) was closer to the decomposition of urethane bonds, whereas the T_d

at 50% weight loss (T_{d50}) was mostly correlated with the degradation of polyurea linkages and polyol bonds. In either case, the degradable behaviors of soy-based PU foam are very similar to the hydrolysis of petro-based foams (Dai et al. 2002; Gerlock et al. 1980). The T_{d50} was expected to increase from 415°C to 440°C with the increase of H_2O from 4.7 to 8.0php due to more polyurea and polybiuret generated (Li et al. 2006). However, there was almost no change from the T_{d5} of neat foams in Table 2, which demonstrated that H_2O was used to build polyurea and polybiuret adducts in a sprayed fast foaming procedure. Alternatively, the urethane formations would not benefit from the increase of H_2O. The increase of Td_{50} indicated that more H_2O blown PU spray foam had higher thermal stability (Thirumal et al. 2008). Urea adducts have been reported to be more thermally stable than urethane structures (Banik and Sain 2008).

Table 2. Effect of H_2O on Cell Thermal Degradation

H_2O, php	Td_5, °C	Td_{50}, °C
4.7	254	415
5.3	257	416
6.7	254	429
8.0	259	440

Wood fibers will start to decompose at 200°C (Kim et al. 2005) and showed two distinct stages with maximum weight loss at 328°C and 445°C in Fig. 6. Wood fiber was completely decomposed at 445°C. So, the foams were exposed to the low temperature thermal decomposition of wood fiber. However, the degradable pattern was variable due to the –OH groups of wood fiber reacting with –NCO groups of PMDI in exothermal reactions.

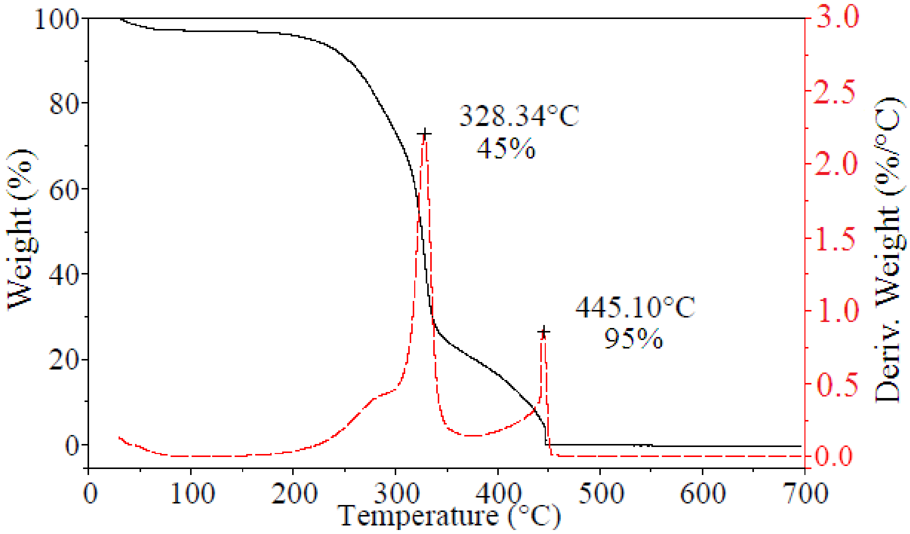

Fig. 6. TGA curve of pure wood fiber (20-35 mesh)

Effect of fiber concentration on foam thermal properties

The pattern of the decomposition of the fiber-reinforced PU spray foam showed that there was also two-stage weight loss behavior accompanied with two endothermic peaks, as shown in Fig. 7. These indicated the thermal decomposition of PU foams consisted of a two-stage degradation of urethane adducts and polyurea bonds. But, this degradable pattern shifted to higher temperature with the increase of fiber. It demonstrated that the employment of wood fiber had important influence on thermal behaviors. The thermal degradation temperature observed from TGA analysis was reported in Table 3.

Different structures had different degradation temperatures, which were portrayed by their break-off peaks. According to Fig. 7, the amount of fiber had significant effects on the thermal decomposition. When a lesser amount of fiber was introduced, it had little effect on the foam decomposition. But, this improvement was enhanced when a high content of fiber was present. The employment of wood fiber alleviated the creaming reaction, which was expected to form more urethane adduct formations because the tertiary amine significantly promoted the polyol-urethane reaction after the fast blowing reaction caused by diamine. In addition, the extra hydroxyl groups in wood fiber were also involved in the urethane reaction.

Afterwards, the T_{d5} increased because the initial stage of weight loss was dominated by the urethane-urea blocks and wood fiber degradation from 300ºC. Still, the delayed gelation time and extended cure time were purposed to contribute PU foam with more trimerization opportunities, exhibiting high T_{d50}, which governed the second stage around 500ºC.

The enhancement of T_{d5} and T_{d50} indicated that the fibers contributed PU spray foam with superior thermal stability. Alternatively, the functions between the reactive –OH groups containing wood fiber and PMDI contributed more thermally stable structures by reacting chemically and extending post-curing time.

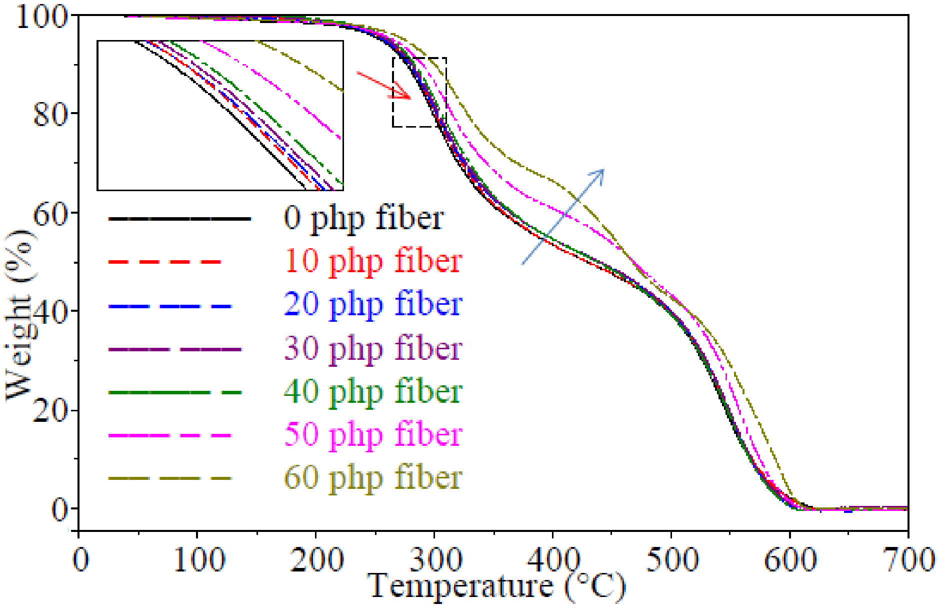

Fig. 7. Effect of fiber concentration on thermal behavior of PU spray foams

Table 3. Effect of Fiber Concentration on Cell Thermal Degradation

35-70 mesh fiber, php	Td_5, ºC	Td_{50}, ºC
0	254	429
10	258	429
20	256	439
30	260	437
40	262	437
50	265	468
60	274	467

Effect of fiber size on foam thermal properties

TGA data were measured using six consecutive fiber lengths. The T_d varied with the fiber particle size, which was seen in Fig. 8. It was observed that the PU spray foam with long fiber had higher thermal stability; this was attributed to the fact that long fiber contained more –OH groups to form complex network structures, exhibiting higher crosslinks. Short fiber will decrease the actual contact surface of the fibers with the foam matrix, leading to less complex structures formed as well as its length. To verify the above observations, the thermal degradation at 5% and 50% were recorded in Table 4. The T_{d50} decreased from 443ºC to 410ºC when the fiber length decreased from 1.04 mm (20-35 mesh) to 0.175 mm (200-325 mesh). Moreover, their relationship was very delicate. Unlike the effect of fiber content, the fiber particle size had little influence on the T_{d5}. This finding proved that wood fibers were involved in building high thermal stability structures regardless of their length. In addition, the cut fiber particles had more primary hydroxyl groups exposed to the foam matrix and functioned as a chain extender.

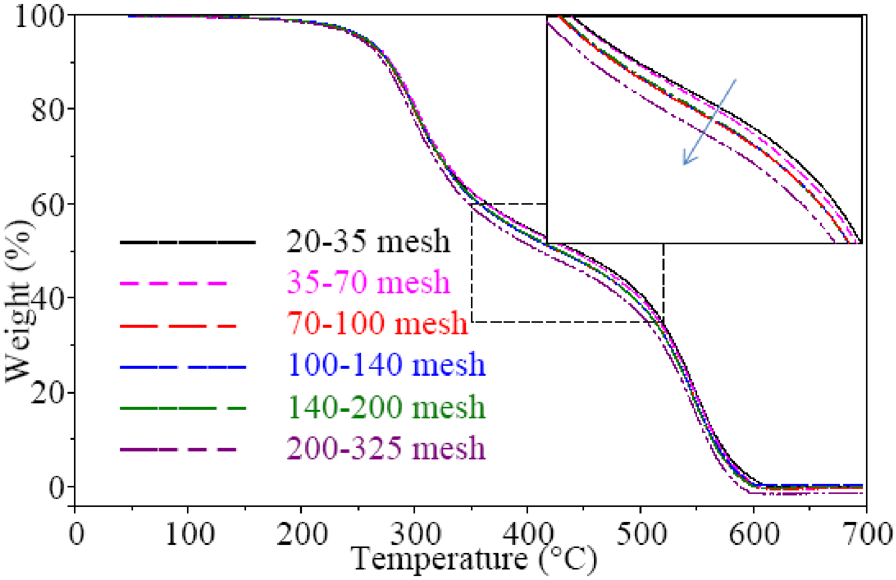

Fig. 8. Effect of fiber size on thermal behavior of PU spray foams

Table 4. Effect of Fiber Particle Size on Cell Thermal Degradation

Fiber particle size, 20php	Td$_5$, ºC	Td$_{50}$, ºC
20-35	255	443
35-70	256	439
70-100	255	426
100-140	256	427
140-200	256	429
200-325	251	410

Mechanical Properties of PU Spray Foams

Foam cell morphology has direct influence on foam mechanical properties, such as compressive strength and tensile strength. Good cellular structure helps in dispersing tension under compression and the applied stress. In our case, H_2O blown PU spray foam had fine cell structure (see Fig. 9a). With the increase of H_2O amount, the compressive strength had a linear increase. The cell walls of neat H_2O blown foam were thinner with the increase of H_2O concentration. This nature of the cell walls could not bear the tensile stress and broke, which led to a loss in tensile strength as shown in Fig. 10.

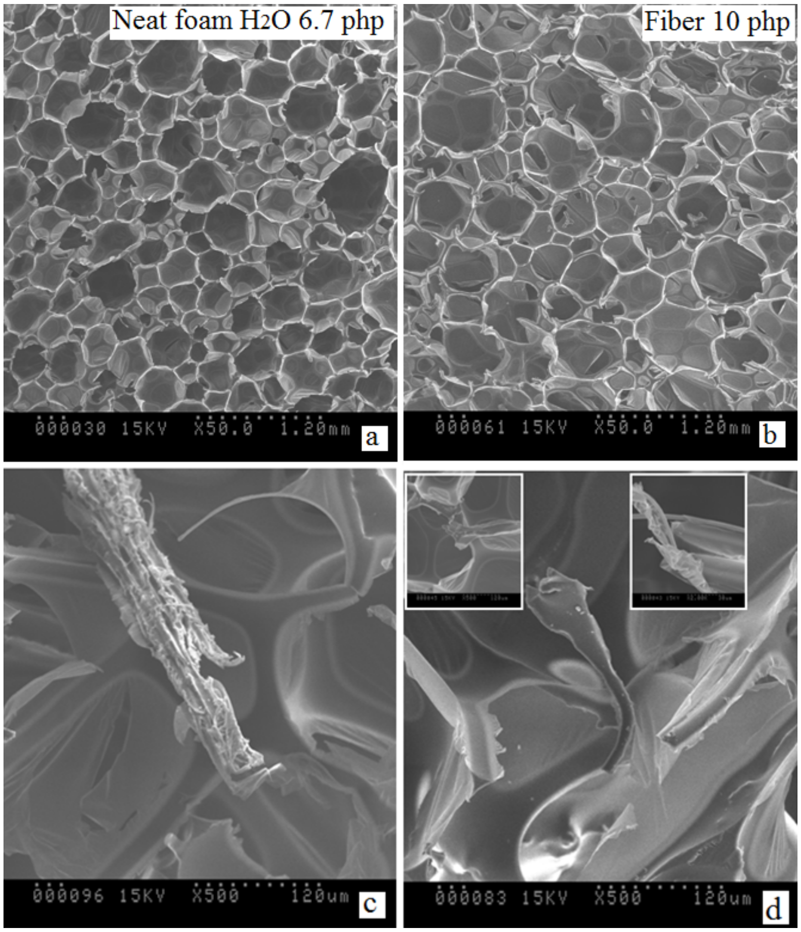

Fig. 9. Three-dimensional cell structures: a - neat PU spray foam; b- 20php fiber reinforced PU spray foam; c-fiber isolation in cells; d-struts disconnection due to fibers

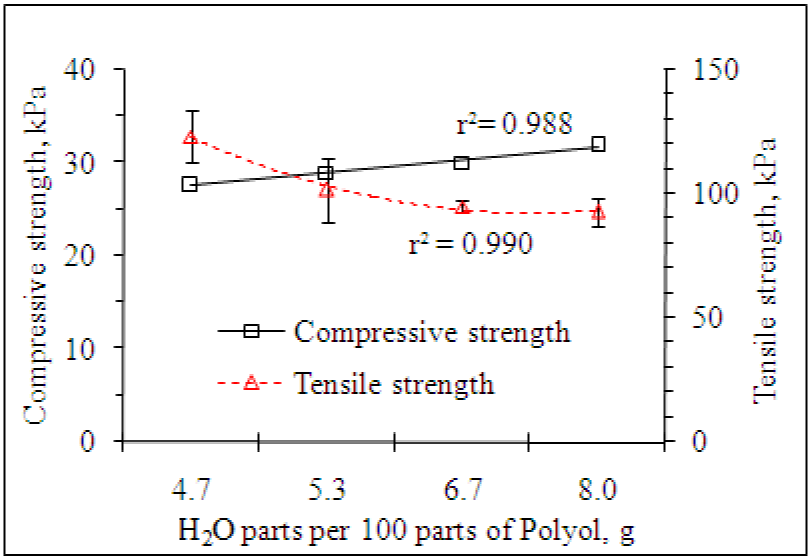

Fig. 10. Effect of H_2O on foam mechanical properties

Although a small amount of fiber will not destroy the whole cell structure (see Fig. 9b), some stiff fibers still perforated the cell walls (Fig. 9c) and also built disconnected struts (Fig. 9d). The fiber reinforced PU spray foam had inferior compres-sive strength at low fiber quantities comparing to neat foam, where the compressive strength decreased from 30 kPa for neat foam down to 20 kPa for the foam with 10php fiber. On the other hand, the stiff fibers also interfered with the cell nodes (see Fig. 11) by framing into the struts,

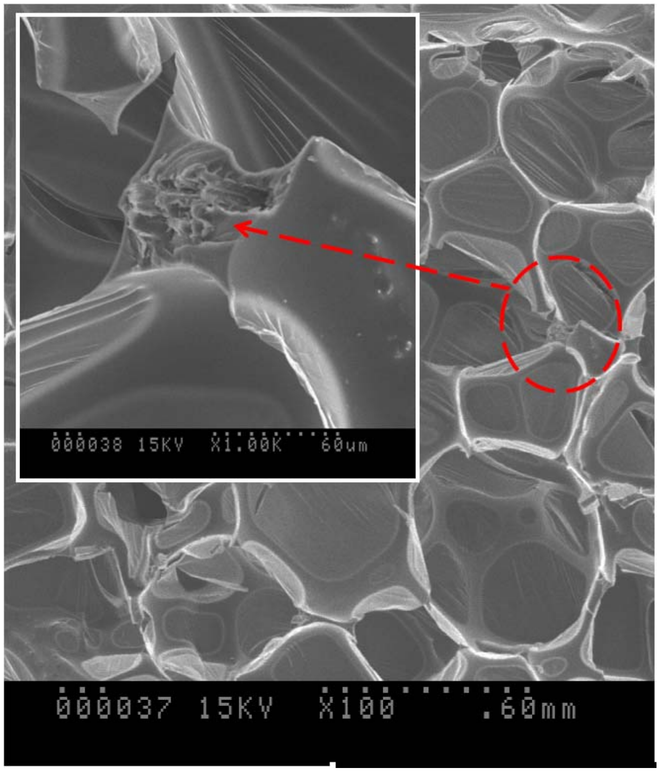

Fig. 11. Fiber framed in cell struts

even though the frames of the cells were not uniform according to its increased foam density and cell size. Therefore, as more fiber was introduced, they provided stiffer cusps to bear high compressive stress, exhibiting superior compressive strength, as shown in Fig. 12. This finding in soy-based PU spray foams corresponds to the behaviors of conventional PU foams with introduction of fiber residue, reported by Silva et al. (2010).

Unlike PU resin composites, PU spray foams have different reinforcement behaviors because a high hydroxyl value polyol in PU resin composites leads to better bond strength (Desai et al. 2003). Obviously that –NCO groups of PMDI will react with primary –OH groups in polyol with priority (Ionescu et al. 2008), and then react with secondary –OH groups on the fiber surface (Pigman and Wolfrom 1948). Thus, wood fiber can interfere with the reaction between polyol and PMDI. Moreover, the stiff fibers destroyed the cell structures (Fig. 9c-d), leading to the decrease of the tensile strength as soon as a small amount of fiber was presented. The value of the tensile strength decreased from 95 kPa for neat PU spray foam to 70 kPa as 10php fiber was employed. Furthermore, the tensile strength continued to decrease as more fiber was introduced after temporary improvement (Liu et al. 2009). Clearly, the destructive effect of wood fiber on cell morphologies was determined by its amount.

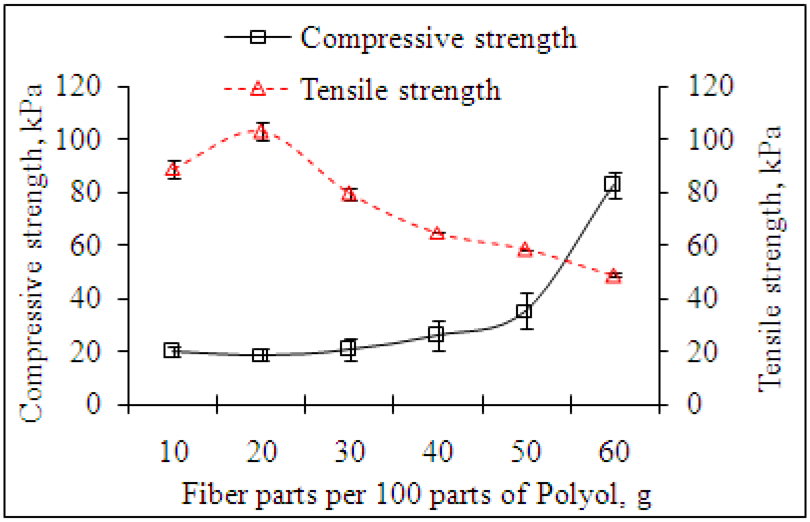

Fig. 12. Effect of fiber concentration on foam mechanical properties

Maximum compressive stresses at 10% deformation for six select fiber particles are recorded at 20php fiber loading in Fig. 13. The trend of compressive strength decreased in a linear relationship thereafter. The compressive strength decreased by 47% from 20.6 kPa for the 20-35 mesh fiber to 10.9 kPa for the 200-325 mesh fiber. Therefore, PU spray foam with 20-35 mesh fiber showed a superior compressive strength. In addition to the compressive strength, a similar trend was also observed in the tensile strength curve.

Although the refined fiber particles have high surface area to expose more –OH groups in wood fiber to the foam matrix, the fiber size greatly affects the mechanical properties of foams. The reinforced foam had achieved an inferior tensile strength (89kPa) due to the destructive effect of fiber by isolation in the foams as described in Fig.

9c. Like a chain extender, 20-30 mesh fiber would be expected to contribute to three-dimensional structures as well as seemingly high crosslinks exceptional to the above-mentioned destructions. Consequently, 35-70 mesh fiber produced superior tensile strength at the value of 103 kPa from its moderate length and better cell morphologies. Actually, very small fiber particles will be powdered as a nucleation agent to create more effective nucleation sites (Guo et al. 2008). So, it was assumed that the shortest fibers acted as a nucleation agent rather than extenders. Spray foams with the shortest fibers had more cells expand more rapidly and melt into large microvoids easily, leading to inferior tensile strength.

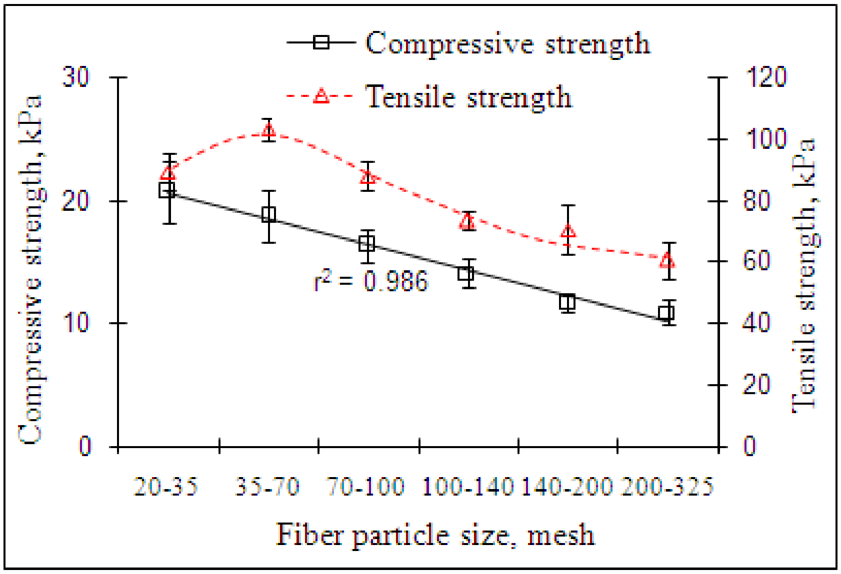

Fig. 13. Effect of fiber particle size on foam mechanical properties

CONCLUSIONS

The amount of water present during foam preparation affected the cell thermal stability by forming more urea/biuret adducts. Still, more urea/biuret structures increased the hard phases in the foams, exhibiting high compressive strength but inferior tensile strength because of poor cell quality.

The amount of fiber had significant effects on foam qualities. As more fiber was introduced, the foam had inferior in tensile strength. However, due to the fibers framing in the cusps and forming three-dimensional structures, the PU spray foam with high fiber content had superior compressive strength. Meanwhile, the fiber reinforced PU spray foam had better thermal stability following the increase of fiber according to their TGA results. Long fiber showed better comparative properties, to short fiber, by acting as a chain extender, which contributed to foam having an improved thermal stability.

ACKNOWLEDGEMENTS

The authors would like to thank the NSERC-CRD and FPInnovations for the financial support. We would also thank Air Products and Chemicals Inc., Huntsman, and Urethane Soy Systems for their donations of materials.

REFERENCES CITED

Banik, I., and Sain, M. M. (2008). "Water blown soy polyol-based polyurethane foams of different rigidities," *Journal of Reinforced Plastics and Composites* 27(4), 357-373.

Bomberg, M. T., and Kumaran, M. K. (1999). "Use of field-applied polyurethane foams in building," Construction Technology Updates No. 32, Published by Institute for Research In Construction, National Research Council of Canada.

Dai, Z., Hatano, B., Kadokawa, J., and Tagaya, H. (2002). "Effect of diaminotoluene on the decomposition of polyurethane foam waste in superheated water," *Polymer Degradation and Stability* 76(2), 179-184.

Desai, S. D., Patel, J. V., and Sinha, V. K. (2003). "Polyurethane adhesive system from biomaterial-based polyol for bonding wood," *International Journal of Adhesion and Adhesives* 23(5), 393-399.

Falke, P., Rotermund, I., Schmutzer, K., and Schmaler, K. (2001). "Production of sound-damping and energy-absorbing polyurethane foams," *US Patent. No. 6316514*. Issued on 13 November 2001.

Gerlock, J. L., Braslaw, J., Mahoney, L. R., and Ferris, F. C. (1980). "Reaction of polyurethane foam with dry steam: Kinetics and mechanism of reactions," *Journal of Polymer Science: Polymer Chemistry Edition* 18(2), 541-557.

Grünbauer, H. J. M., Thoen, J. A., Folmer, J. C. W., and Van Lieshout, H. C. (1992). "Polymer morphology of water-blown rigid polyurethane foam: Development of new polyols," *Journal of Cellular Plastics* 28(2), 36-47.

Guo, G., Lee, Y. H., Rizvi, G. M., and Park, C. B. (2008). "Influence of wood fiber size on extrusion foaming of wood fiber/HDPE composites," *Journal of Applied Polymer Science* 107(6), 3505-3511.

Hsueh, C.-H. (1989). "Analytical analyses of stress transfer in fibre-reinforced composites with bonded and debonded fibre ends," *Journal of Materials Science* 24(12), 4475-4482.

Ionescu, M., Petrović, Z. S., and Wan, X. (2008). "Primary hydroxyl content of soybean polyols," *Journal of The American Oil Chemists' Society* 85(5), 465-473.

Javni, I., Zhang, W., and Petrović, Z. S. (2004). "Soybean-oil-based polyisocyanurate rigid foams," *Journal of Polymers and the Environment* 12(3), 123-129.

Khazabi, M., Gu, R., and Sain, M. (2011). "Fiber reinforced soy-based polyurethane spray foam insulation. Part 1: Cell morphologies," *BioResources* 6(4), 3757-3774.

Kim, H.-S., Yang, H.-S., Kim, H.-J., Lee, B.-J., and Hwang, T.-S. (2005). "Thermal properties of agro-flour-filled biodegradable polymer bio-composites," *Journal of Thermal Analysis and Calorimetry* 81(2), 299-306.

Li, X., Cao, H., and Zhang, Y. (2006). "Structures and physical properties of rigid polyurethane foams with water as the sole blowing agent," *Science in China series B: Chemistry* 49(4), 363-370.

Liu, Z., Yu, F., Fang, G., and Yang, H. (2009). "Performance characterization of rigid polyurethane foam with refined alkali lignin and modified alkali lignin," *Journal of Forestry Research* 20(2), 161-164.

Moore, S. E., and Ference, D. M. (1998). "Polyurethane system optimization for energy efficiency," *Journal of Cellular Plastics* 34(2), 183-194.

Petrović, Z. S. (2008). "Polyurethanes from vegetable oils," *Polymer Reviews* 48(1), 109-155.

Pollack, J. W. (2004). "Soy vs. petro polyols, a life cycle comparison," *GPEC 2004 Paper #37*, Omni Tech International, Ltd.

Pigman, W. W., and Wolfrom, M. L. (1948). *Advances in Carbohydrate Chemistry*, Academic Press Inc. New York, NY, USA, 3, 191.

Saber, H. H., Kashef, A., Bwalya, A., and Lougheed, G. (2010). "Numerical and experimental investigations of fire behavior of polyurethane foam and wood cribs in a medium-sized residential room," *Institute for Research in Construction, Natural Research Council Canada*. Research report #RR-291. 8 March 2010.

Silva, M. C., Takahashi, J. A., Chaussy, D., Belgacem, M. N., and Silva, G. G. (2010). "Composites of rigid polyurethane foam and cellulose fiber residue," *Journal of Applied Polymer Science* 117(6), 3665-3672.

Thirumal, M., Khastgir, D., Singha, N. K., Manjunath, B. S., and Naik, Y.P. (2008). "Effect of foam density on the properties of water blown rigid polyurethane foam," *Journal of Applied Polymer Science*, 108(3), 1810-1817.

USDA: Foreign Agricultural Service. (2011). "Oilseed: World markets and trade," June 2011 data.

Article submitted: June 12, 2011; Peer review completed: July 23, 2011; Revised version received and accepted: August 4, 2011; Published: August 6, 2011.